Geoscience Frontiers xxx (2016) 1–12

HOSTED BY

ELSEVIER

Contents lists available at ScienceDirect

China University of Geosciences (Beijing)

Geoscience Frontiers

journal homepage: www.elsevier.com/locate/gsf

Research paper

Uncertainty of soil erosion modelling using open source high resolution and aggregated DEMs

Arun Mondal [a,*], Deepak Khare [a], Sananda Kundu [a], Sandip Mukherjee [b], Anirban Mukhopadhyay [c], Surajit Mondal [d]

[a] Department of Water Resources Development & Management, Indian Institute of Technology, Roorkee, India
[b] Department of Natural Resources, TERI University, New Delhi 110 070, India
[c] School of Oceanographic Studies, Jadavpur University, Kolkata, India
[d] Division of Land & Water Management, Research Complex for Eastern Region (RCER), Indian Council of Agricultural Research (ICAR), Patna, India

ARTICLE INFO

Article history:
Received 18 December 2015
Received in revised form
24 February 2016
Accepted 2 March 2016
Available online xxx

Keywords:
DEM
RUSLE
SRTM
ASTER
CARTOSAT

ABSTRACT

Digital Elevation Model (DEM) is one of the important parameters for soil erosion assessment. Notable uncertainties are observed in this study while using three high resolution open source DEMs. The Revised Universal Soil Loss Equation (RUSLE) model has been applied to analysis the assessment of soil erosion uncertainty using open source DEMs (SRTM, ASTER and CARTOSAT) and their increasing grid space (pixel size) from the actual. The study area is a part of the Narmada river basin in Madhya Pradesh state, which is located in the central part of India and the area covered 20,558 km^2. The actual resolution of DEMs is 30 m and their increasing grid spaces are taken as 90, 150, 210, 270 and 330 m for this study. Vertical accuracy of DEMs has been assessed using actual heights of the sample points that have been taken considering planimetric survey based map (toposheet). Elevations of DEMs are converted to the same vertical datum from WGS 84 to MSL (Mean Sea Level), before the accuracy assessment and modelling. Results indicate that the accuracy of the SRTM DEM with the RMSE of 13.31, 14.51, and 18.19 m in 30, 150 and 330 m resolution respectively, is better than the ASTER and the CARTOSAT DEMs. When the grid space of the DEMs increases, the accuracy of the elevation and calculated soil erosion decreases. This study presents a potential uncertainty introduced by open source high resolution DEMs in the accuracy of the soil erosion assessment models. The research provides an analysis of errors in selecting DEMs using the original and increased grid space for soil erosion modelling.

1. Introduction

Soil erosion is one of the major environmental hazards which leads to the loss of fertility and reduced agricultural production and creates problems in the ecosystem worldwide. Erosion is very high in Asia, Africa and South America and the rate of erosion varies from 30 to 40 t ha^{-1} yr^{-1} (Barrow, 1991). In India, the rate of soil erosion is about 16.40 t ha^{-1} yr^{-1} (Narayana and Babu, 1983). Soil erosion estimation of a study area has limitations if done only by field based studies because of the complexity of the earth surface that governs the soil erosion process (Saha and Pande, 1993). Geoinformatics tools can assess the erosion process considering complex earth surface in spatial aspect. Rate of soil erosion varies because of changes in elevation, soil type, land use/land cover, rainfall, etc. (Mallick et al., 2014).

Digital Elevation Model (DEM) is a continuous surface of the elevation from which terrain attributes (slope, aspect, curvature, topographic index, drainage area and network) are extracted (Mukherjee et al., 2013a). It is one of the important parameters for estimating soil erosion. DEM is generated by different techniques, such as, photogrammetric method (Hohle, 2009), interferometry (Kervyn, 2001), airborne laser scanning (Favey et al., 2003), aerial stereo photograph (Schenk, 1996), topographic surveys (Wilson and Gallant, 2000). DEM involves different types of errors and accuracy with varying terrain conditions. Accuracy of DEM can be influenced by the accuracy of the soil erosion modelling outputs. Few studies related to the accuracy of the DEM with different grid

* Corresponding author.
E-mail address: arun.iirs@gmail.com (A. Mondal).
Peer-review under responsibility of China University of Geosciences (Beijing).

http://dx.doi.org/10.1016/j.gsf.2016.03.004

space (original or increased) are observed in the works of Chaplot (2005) and Mukherjee et al. (2013a, b).

Identification of soil erosion status has been studied by many researchers (Alice and Christian, 2003; Fu et al., 2005; Xu et al., 2007; Dabral et al., 2008; Feng et al., 2010; Chen et al., 2011; Hasan et al., 2013; Pan and Wen, 2014) using geoinformatics techniques in spatial domain. The higher rate of erosion was observed in some studies in Indian condition (Jain et al., 2001; Pandey et al., 2007; Dabral et al., 2008; Prasannakumar et al., 2012). For the improvement of the accuracy level for estimation of soil erosion, DEMs with higher accuracy are used by Lin et al. (2013), Prasuhn et al. (2013) and Quiquerez et al. (2014).

Some well known established models for estimating soil erosion are MMF (Morgan Morgan Finney) by Jain et al. (2001), USLE (Universal Soil Loss Equation) by Pandey et al. (2007), Mondal et al. (2014), MUSLE (Modified Universal Soil Loss Equation) by Lin et al. (2013), RUSLE (Revised Universal Soil Loss Equation) by Mallick et al. (2014). The RUSLE model is more efficient, robust and

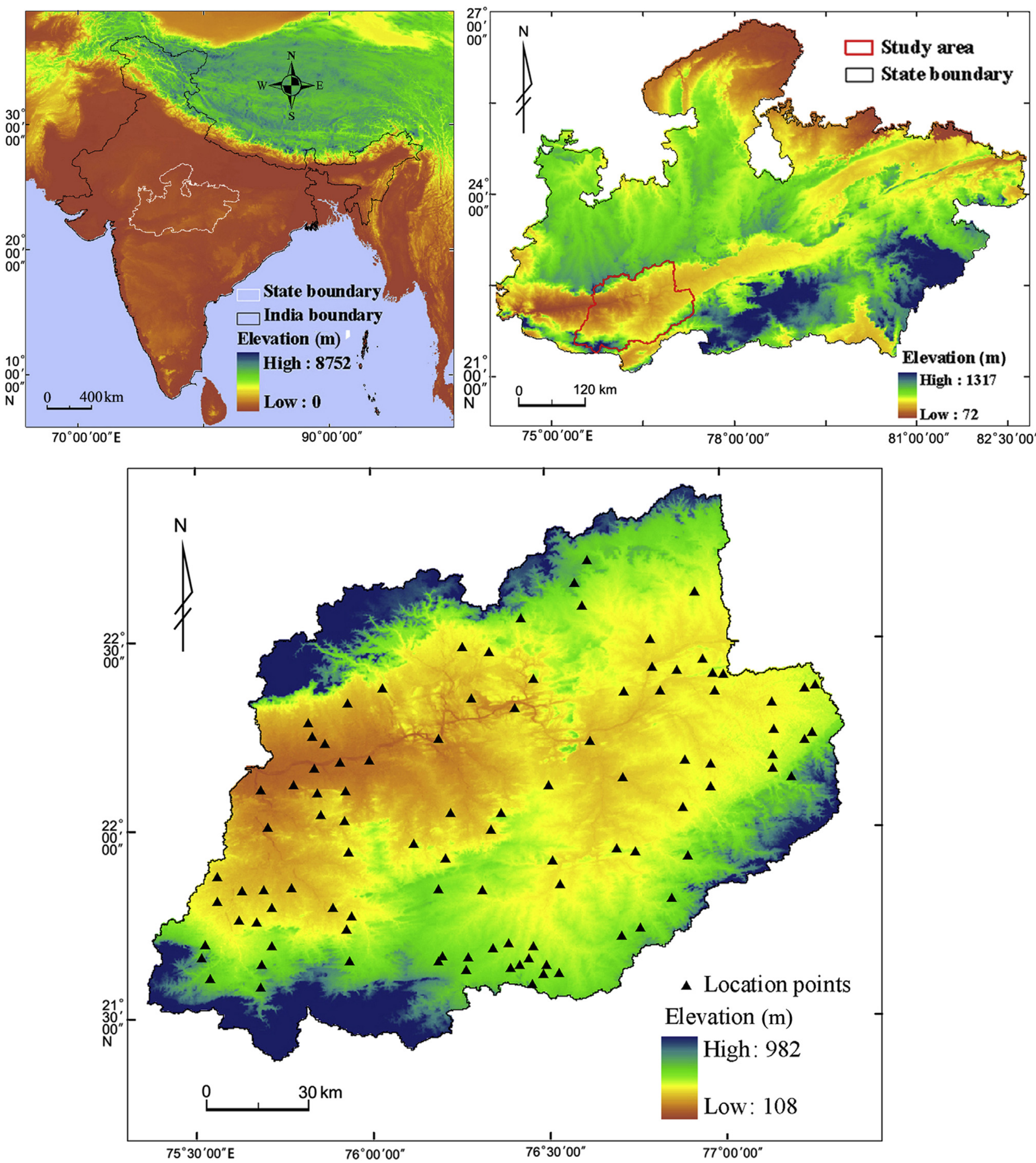

Figure 1. Study area map showing the distribution of selected location of actual elevation from Mean Sea Level (MSL) over digital elevation model (DEM) of ASTER in central part of India.

Please cite this article in press as: Mondal, A., et al., Uncertainty of soil erosion modelling using open source high resolution and aggregated DEMs, Geoscience Frontiers (2016), http://dx.doi.org/10.1016/j.gsf.2016.03.004

Table 1
Used data and their details.

Sl. no.	Extracted parameters	Data	Year	Vintage resolution	Sources
1	Soil type	Soil map	1999	1:250,000	National Bureau of Soil Survey and Land Use Planning (NBSS & LUP), India
2	Land use and NDVI	LISS-III images	2011 (Seasonal)	30 m	National Remote Sensing Centre, India
3	Validation	Sediment load	2009	NA	Central Water Commission (CWC), India
4	LS and slope	DEM types			
		(1) SRTM	(1) 2015	(1) 30 m	(1) http://earthexplorer.usgs.gov/
		(2) CARTOSAT	(2) 2014	(2) 30 m	(2) http://bhuvan.nrsc.gov.in/bhuvan_links.php
		(3) Aster	(3) 2011	(3) 30 m	(3) http://earthexplorer.usgs.gov/
5	Rainfall	Daily rainfall	2009	NA	Indian Meteorological Department (IMD)
6	Elevation	Toposheet	1977	1:50,000	Survey of India (SOI)

simple, but the user should be concerned about proper extrapolation, spatial scale effects and the complexity of the erosion process (Li et al., 2011). Liu et al. (2011) showed the change effects of the LiDAR grid space on the uncertainty of soil erosion by USLE model, and Lin et al. (2013) used two DEMs (ASTER in 30 m and SRTM in 90 m) to estimate the uncertainty of soil erosion by MUSLE model. Mondal et al. (2016) presented the uncertainty of soil erosion by RUSLE model using original resolution of open source of DEMs (GTOPO30, SRTM, ASTER and CARTOSAT DEM). However, all the aboved studies showed that there is a lack of work in the field of uncertainty analysis of different DEMs with original and aggregated resolutions and their impact on the RUSLE soil erosion modelling. Use of different types of open source DEMs (SRTM, ASTER and CARTOSAT) with the original resolution (30 m) and aggregated resolution has a scope to identify the uncertainty of soil erosion modelling by RUSLE model, considering the changes in relation to the elevation accuracy. The results show significant variation in the rate of soil erosion only by using different DEMs of the same resolution and then by aggregating the resolution of all DEMs.

The objective of this study is to assess the impacts of different resolutions (original and aggregated grid space) of open source DEMs (SRTM, ASTER and CARTOSAT) on soil erosion by Revised Universal Soil Loss Equation (RUSLE) model. Some actual elevation points are used to compare with different types of DEMs to check the accuracy after converting height data to the same datum. DEMs with various grid spaces are used to estimate different soil erosion rates and amounts, and are compared with the observed sediment yield data of the study area.

2. Study area

A part of the Narmada River basin is taken as the study area, which is situated in the districts of Harda, Dewas, East Nimar (Khandwa) and West Nimar (Khargone) in Madhya Pradesh of central India. The area is geographically located between 21°23′7.7″N to 22°55′08″N and 75°21′07″E to 77°21′17″E and covers 20,558 km^2 of area (Fig. 1). The subtropical climate of the study area is characterized by hot and dry summer season (March–May), monsoonal rains (June–October), and cool dry winter months (November–February). Mean annual rainfall is about 1370 mm, which is spatially decreasing from east to west (Mondal et al., 2014). Main river is located at the middle part of the study area flowing from east to west. The higher elevated area is situated in the northern and southern boundary. Elevation ranges from 108 to 982 m and the mean value is 328.66 m. The areal distribution of the less than 2° slopes is 48.39%, 2° to 5° is 36.07%, 6° to 10° is 10.38% and more than 10° slope cover about 5.18% (Aster DEM).

3. Data and methodology

Details of various data used in the soil erosion modelling, are given in the Table 1. The SRTM DEM is recently published with 30 m grid space which is prepared by the interferometry method. The ASTER and CARTOSAT are taken from the recently published data (ASTER v002 and CARTOSAT v3R1), which are prepared using stereo-pairs of satellite imagery. DEMs with drainage maps are shown in a part of the study area, which indicate a similar pattern of distribution of drainages and less variation among them (Fig. 2).

Linear Imaging Self Scanning Sensor (LISS-III) is geometrically corrected with reference to the toposheet. DEMs and soil map are corrected using toposheet and LISS-III imageries. All spatial maps are transferred into the same projection and the datum type is given as the UTM (Universal Transverse Mercator) projection zone 45 North and WGS 84 (World Geodetic System 1984). The EGM96 surface is a vertical datum, which is very close to the local datum of MSL (Mean Sea Level) for India (Sun et al., 2003; Mukherjee et al., 2013b). Vertical datum of all DEMs is converted into EGM96 for

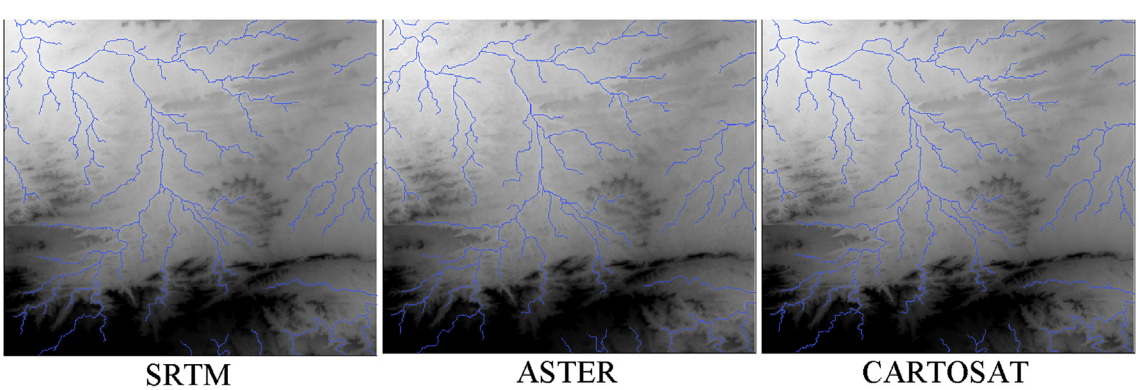

Figure 2. SRTM, ASTER and CARTOSAT DEM map in part of the study area.

comparing the accuracy level with respect to the toposheet height (MSL datum) (http://earth-info.nga.mil/GandG/wgs84/gravitymod/egm96/intpt.html).

Actual heights of the locations are identified from the toposheet and are compared with the corresponding DEMs' heights (different grid space) to analyse the change pattern of the elevations with accuracy. The soil erosion rate is estimated by the RUSLE model using cover management factor (C), soil erodibility factor (K), rainfall erosivity factor (R), topographic factor (LS) and conservation supporting practice (P). Various LS factors are calculated using various grid spaces of DEMs to evaluate the change in the soil erosion rate with accuracy (Fig. 3). Three DEMs are aggregated into different grid spaces. The grid spaces are considered to be of six types ($30 \times 1 = 30$ m, $30 \times 3 = 90$ m, $30 \times 5 = 150$ m, $30 \times 7 = 210$ m, $30 \times 9 = 270$ m and $30 \times 11 = 330$ m) shown in Fig. 4. The point sediment yield data of 2009 is used here controlled by CWC (Central Water Commission) under the Govt. of India. Frequency of data is daily time interval.

3.1. Soil erosion

3.1.1. Revised Universal Soil Loss Equation

The soil erosion modelling by RUSLE (Revised Universal Soil Loss Equation) is a modified form of the USLE (Renard et al., 1991). RUSLE is expressed as

$$A = R \times K \times LS \times C \times P \quad (1)$$

where, A is the annual rate of soil loss (t ha^{-1} yr^{-1}), R is the rainfall erosivity (MJ mm ha^{-1} h^{-1} yr^{-1}), K is the soil erodibility (t ha h ha^{-1} MJ^{-1} mm^{-1}), LS is the topographic factor stated as slope length and steepness, C is the factor for crop management and P stands for conservation supporting practice.

3.1.2. Rainfall erosivity factor (R)

Due to lack of hourly intensity data, monthly and annual rainfall data are used to calculate the R-factor using the following equation by Wischmeier and Smith (1978):

$$R = \sum_{i=1}^{12} 1.735 \times 10^{1.5\log_{10}(P_i^2/P) - 0.08188} \quad (2)$$

where, R is the rainfall erosivity factor (MJ mm ha^{-1} h^{-1} yr^{-1}), P_i is the monthly rainfall (mm), P is the annual rainfall (mm).

In Indian condition, this model has been used by Dabral et al. (2008) and Pandey et al. (2009) in northeastern India and Himalayan watershed respectively.

3.1.3. Soil erodibility factor (K)

The K-factor is calculated using the following equation (Wischmeier and Smith, 1978; Adhikary et al., 2014):

$$K = \frac{1}{759}\left\{2.1 \times 10^{-4} \times M^{1.14}(12 - a) + 3.25(b - 2) + 2.5(c - 3)\right\} \quad (3)$$

where, K is soil erodibility factor (t ha h ha^{-1} MJ^{-1} mm^{-1}), M is the particle size parameter (% silt + % very fine sand) × (100 − % clay), a is the organic matter content (%), b is the soil structure code, c is the soil permeability class. The data is taken from the soil series book of Madhya Pradesh state (NBSS, 1996, 1999).

3.1.4. Topographic factor (LS)

The L factor is calculated by the following equation (McCool et al., 1987):

$$L = \left(\frac{\lambda}{22.1}\right)^m \quad (4)$$

where, L is the slope length factor, λ is the field slope length (m), and m is the dimensionless exponent depending on the slope steepness, which is 0.5 for slopes exceeding 5%, 0.4 for 4% slopes and 0.3 for less than 3% slopes. The slope steepness factor (S) is computed on the basis of a relationship for the slope length, which is longer than 4 m. The following equations are given for S (McCool et al., 1987):

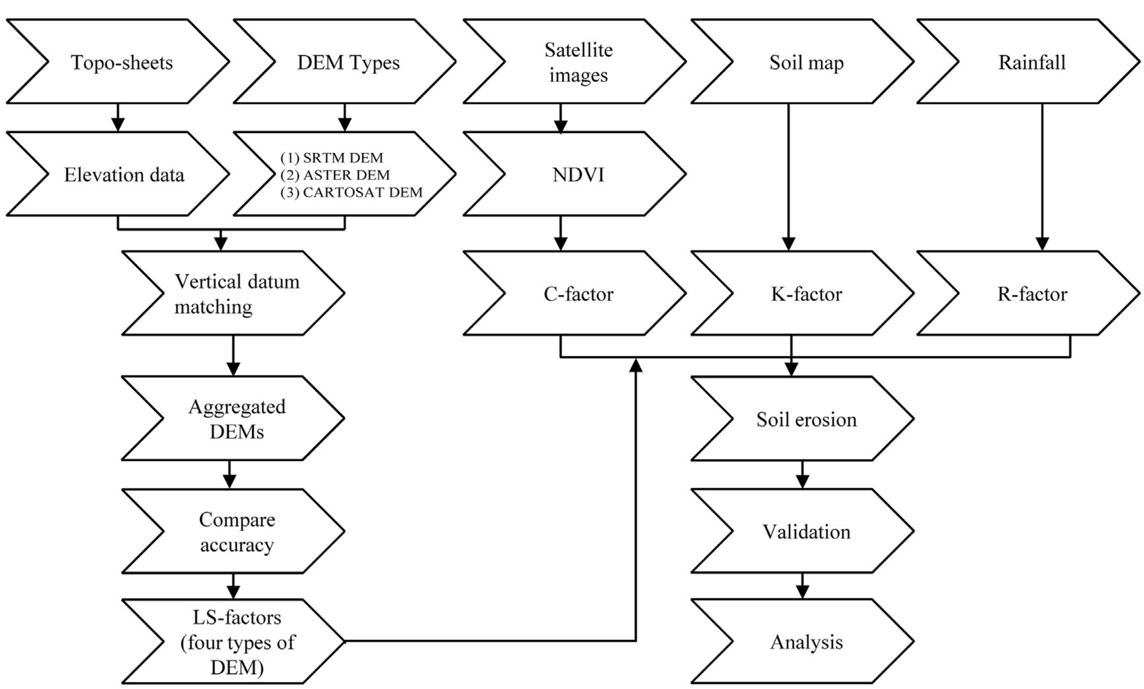

Figure 3. Methodology for uncertainty of soil erosion assessment using three DEMs (SRTM, ASTER and CARTOSAT) with their actual (30 m) and aggregated grid space (90, 150, 210, 270 and 330 m).

a

	1	2	3	4	5	6	7	8	9	10	11
1	551	547	540	533	524	514	504	490	482	478	472
2	561	558	553	544	533	523	515	506	497	498	492
3	564	564	560	552	543	534	528	524	518	513	509
4	562	566	564	556	550	544	541	539	535	530	525
5	557	566	565	563	559	556	553	549	544	538	532
6	552	564	564	566	568	567	561	557	551	542	534
7	546	556	560	565	570	568	563	560	551	543	534
8	541	551	557	562	568	567	562	555	544	536	530
9	537	547	553	561	566	563	555	546	536	530	524
10	537	547	531	538	563	559	552	542	532	524	519
11	541	551	559	565	562	555	549	540	527	519	511

b

	1	2	3
1			
2		555	
3			

c

	1	2	3	4	5
1					
2					
3			553		
4					
5					

d

	1	2	3	4	5	6	7
1							
2							
3							
4				551			
5							
6							
7							

e

	1	2	3	4	5	6	7	8	9
1									
2									
3									
4									
5					548				
6									
7									
8									
9									

f

	1	2	3	4	5	6	7	8	9	10	11
1											
2											
3											
4											
5											
6						543					
7											
8											
9											
10											
11											

Figure 4. Grid space change with value, (a) original 30 m, (b) 90 m (3 grid × 3 grid), (c) 150 m (5 grid × 5 grid), (d) 210 m (7 grid × 7 grid), (e) 270 m (9 grid × 9 grid) and (f) 330 m (11 grid × 11 grid).

$$S = 10.8 \sin\theta + 0.03, \quad S < 9\% \tag{5}$$

$$S = 16.8 \sin\theta - 0.05, \quad S \geq 9\% \tag{6}$$

where, S gives the slope steepness factor and θ denotes the slope angle in degree. The slope steepness factor is considered as dimensionless. The spatial distribution of the topographic factor ranges from 0.03 to 16.43 within the basin area.

3.1.5. Cover management factor (C)

The C value is mainly dependent on the surface cover, vegetation canopy (crop), surface roughness and soil moisture. C is estimated by the NDVI (Normalized Difference Vegetation Index) (Van der Knijff et al., 1999). Van der Knijff et al. (1999) suggested for $\alpha = 1$ and $\beta = 2$.

$$C = \exp\left(-\alpha \times \frac{\text{NDVI}}{\beta - \text{NDVI}} \right) \tag{7}$$

The crop management factor is related to the land use or land cover type of the study area. The C or crop management factor is calculated from the NDVI, derived from the LISS-III images. The value of the conservation practice (P) is taken as 1 for all the land use classes.

3.2. Accuracy assessment

The accuracy status of DEMs is estimated using elevation data by four indices, such as, root mean square error (RMSE) (Kundu et al., 2014; Duhan and Pandey, 2015), normalized mean square error (NMSE) (Duhan and Pandey, 2015), nash-sutcliffe coefficient (NASH) (Nash and Sutcliffe, 1970; Duhan and Pandey, 2015) and correlation coefficient (CC) (Duhan and Pandey, 2015).

(1) Root mean square error $\text{RMSE} = \sqrt{\frac{1}{N}\sum_{i=1}^{N}\left(y_i - \hat{y}_i\right)^2}$

(2) Normalized mean square error

$$\text{NMSE} = \frac{\frac{1}{N}\sum_{i=1}^{N}\left(y_i - \hat{y}_i\right)^2}{(S_{obs})^2}$$

(3) Nash-Sutcliffe coefficient

$$\text{NASH} = 1 - \frac{\frac{1}{N}\sum_{i=1}^{N}\left(y_i - \hat{y}_i\right)^2}{\frac{1}{N}\sum_{i=1}^{N}\left(y_i - \bar{y}_i\right)^2}$$

(4) Correlation coefficient

$$\text{CC} = \frac{N\sum\left(y_i \times \hat{y}_i\right) - \left(\sum y_i\right) \times \left(\sum \hat{y}_i\right)}{\sqrt{\left[N\sum y_i^2 - \left(\hat{y}_i\right)^2\right] \times \left[N\sum y_i^2 - \left(\hat{y}_i\right)^2\right]}}$$

Here, y_i and $\hat{y}_i$ represent actual elevation and elevation from DEMs respectively. N denotes the training and testing sample size. A small value of the RMSE and NMSE indicates less discrepancy between the observed and predicted series, thus provides better

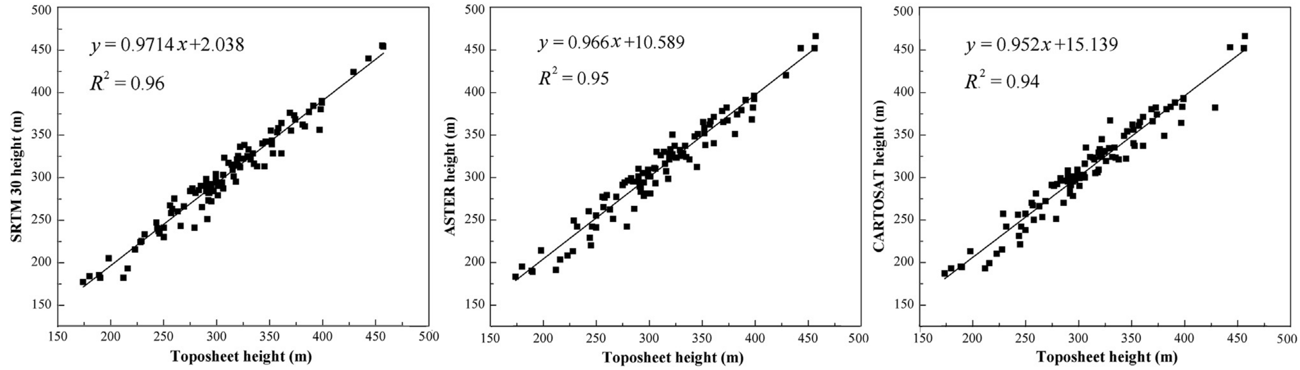

Figure 5. Plot between actual height and DEMs height.

prediction accuracy, while higher values of NASH and CC give better accuracy.

4. Results and discussion

4.1. Accuracy of DEMs

Total 100 points for bench mark and spot height for elevation are taken which are well distributed over the entire study area. Elevation of DEMs has been plotted with actual points by regression lines (Fig. 5). The distribution of the points is found to be located close to the regression line for three DEMs (SRTM, ASTER and CARTOSAT) with the R^2 values 0.96, 0.95 and 0.94 respectively. The probability value is, $p < 0.005$ for Student's t-test and is statistically significant (two-tailed) for all DEMs. Accuracy results are compared and are shown in Fig. 6 by RMSE, NMSE, NASE and CC with different grid spaces of DEMs. RMSE and NMSE values of SRTM are 13.31, 14.51, and 18.19 m and 3.04, 3.32, and 4.25 m in 30, 150 and 330 m grid space respectively, which show that with the coarser resolution, the accuracy decreases. Similarly, in the CARTOSAT DEM, RMSE values are 13.93, 16.14, and 19.05 m, while NMSE values are 3.30, 3.84, and 4.67 m respectively. RMSE and NMSE values of ASTER are observed to be in between the values of SRTM and CARTOSAT. Therefore, the RMSE and NMSE values of SRTM are less in the original and aggregated DEMs than the ASTER and CARTOSAT indicating better accuracy. NASH and CC values have decreased from 0.949 to 0.931 and 0.979 to 0.967 in SRTM and 0.943 to 0.93 and 0.971 to 0.964 in CARTOSAT, while ASTER has shown 0.947 to 0.93 and 0.973 to 0.96 respectively. RMSE and NMSE values are decreasing and NASH and CC values are increasing, when grid space is decreased for three

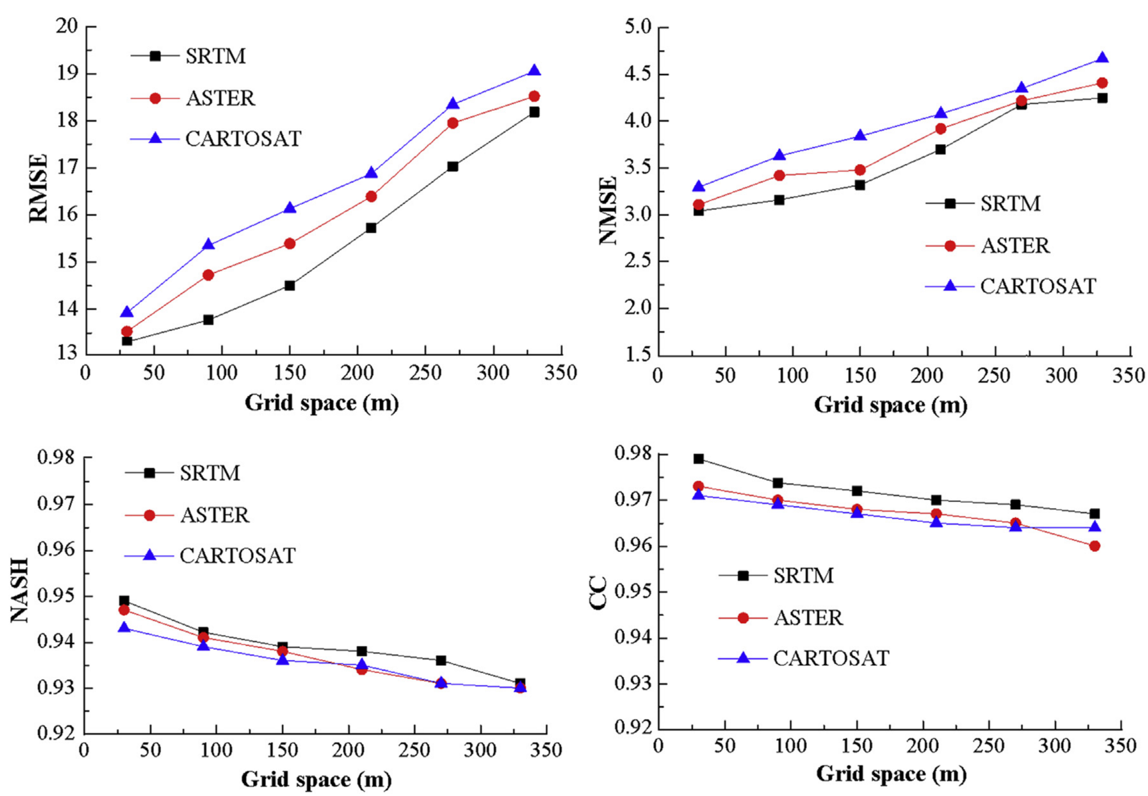

Figure 6. The accuracy assessment calculated by 100 sample points from toposheet.

Please cite this article in press as: Mondal, A., et al., Uncertainty of soil erosion modelling using open source high resolution and aggregated DEMs, Geoscience Frontiers (2016), http://dx.doi.org/10.1016/j.gsf.2016.03.004

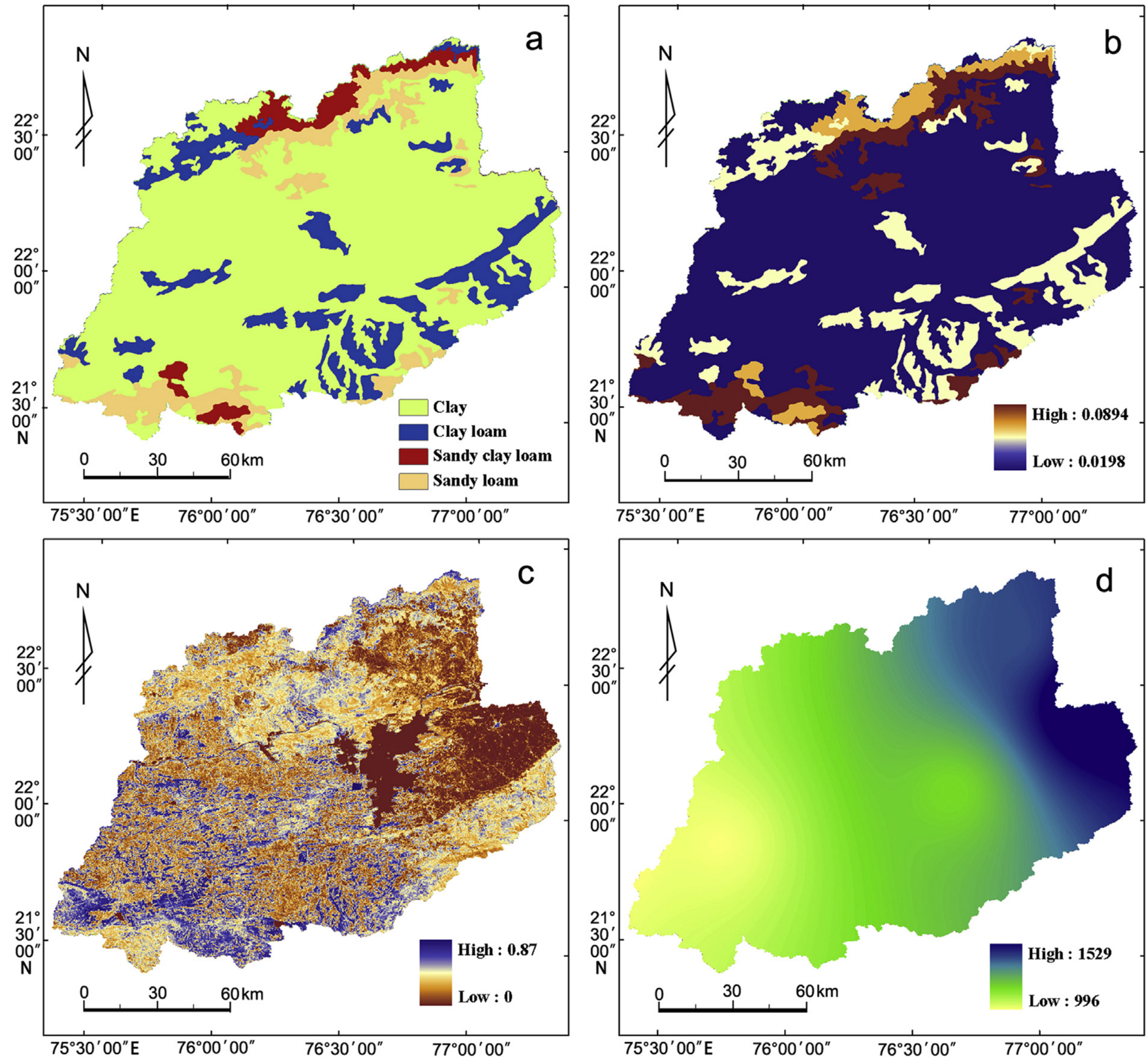

Figure 7. Spatial distribution map of (a) soil, (b) K factor, (c) C factor, (d) R factor.

DEMs. It is indicated that the accuracy of DEMs is decreased when the grid space of DEMs is increased from their actual grid size. But SRTM DEM shows better accuracy among three DEMs, while ASTER and CARTOSAT show low accuracy (Fig. 6).

4.2. Soil erosion

Rainfalls of eight rain gauge stations are taken to calculate the rainfall erosivity (R) and are interpolated by Inverse Distance Weighting (IDW) method to show spatial distribution. Four major types of soils are clay, clay loam, sandy clay loam and sandy loam, where clay soil is covering a maximum area (72.72%) (Fig. 7a). Soil erodibility (K) values are varying from 0.0198 to 0.0894 t ha h ha^{-1} MJ^{-1} mm^{-1} (Fig. 7b). The cover management factor (C) is generated using NDVI (Normalized Difference Vegetation Index) prepared from the satellite imagery. Ranges of C factor vary from 0 to 0.87 in the study area (Fig. 7c). The R or rainfall erosivity value is higher in the eastern part where rainfall is high and it is gradually decreasing from east to west. Range of R values is 996 to 1529 MJ mm ha^{-1} h^{-1} yr^{-1} (Fig. 7d). Topographic factor (LS)

Table 2
Validation and compare of soil erosion.

DEMs	Sedimentation (t yr^{-1})				Change (%)		
	SRTM	ASTER	CARTOSAT	Observed	SRTM	ASTER	CARTOSAT
30 m	19,632,890	19,961,818	19,981,510	19,039,076	3.12	4.85	4.95
90 m	19,096,758	18,805,204	18,367,874		0.30	−1.23	−3.53
150 m	18,535,843	18,097,989	17,718,515		−2.64	−4.94	−6.94
210 m	18,012,887	17,632,745	17,223,361		−5.39	−7.39	−9.54
270 m	17,695,512	17,050,974	16,963,082		−7.06	−10.44	−10.90
330 m	17,105,966	16,608,019	16,783,765		−10.15	−12.77	−11.85

Please cite this article in press as: Mondal, A., et al., Uncertainty of soil erosion modelling using open source high resolution and aggregated DEMs, Geoscience Frontiers (2016), http://dx.doi.org/10.1016/j.gsf.2016.03.004

is prepared using slopes (degree and percentage), which are generated from DEMs. The LS factor is the only changeable parameter in the calculation of soil erosion. Variation in grid spaces of DEMs is used for identifying the changes in the accuracy of soil erosion.

4.3. Comparison of observed and modelled soil erosion

The percentages of change values of sediment yield with respect to the observed are 3.12%, 4.85% and 4.95% of SRTM, ASTER and CARTOSAT respectively, using their actual grid space (30 m) by RUSLE model. Change rates of soil erosion (amount) are 0.30%, −2.64%, −5.39%, −7.06% and −10.15% using SRTM, −1.23%, −4.49%, −7.39%, −10.44% and −12.77% using ASTER, while −3.53%, −6.96%, −9.54%, −10.90% and −11.85% using CARTOSAT with respect to 30, 90, 150, 210, 270 and 330 m grid space respectively. Amount of soil erosion is observed to decrease for all DEMs with the increasing grid space size from the original (Table 2). The SRTM DEM shows little better results compared to ASTER and CARTOSAT using different grid spaces.

The mean elevation value increases from the actual value (30 m grid space) with increasing grid space of DEMs. However, mean LS factor decreases with the decrease of mean slope, when the grid space of DEMs increases. Therefore, the erosion rate decreases due to decrease in the LS factor values. Similarly, SRTM DEM estimates low rate of soil erosion due to low mean elevation, slope and LS values compared to ASTER and CARTOSAT (Fig. 8).

Estimated soil erosion maps are categorized into six classes (<5, 5–10, 11–20, 21–40, 41–80 and >80 t ha^{-1} yr^{-1}). The percentage of area is maximum in <5 t ha^{-1} yr^{-1} category for three DEMs. The affected area is observed to increase gradually due to aggregation or increased grid space of all DEMs. The percentages of area for SRTM, ASTER and CARTOSAT are 58.73%, 61.96% and 56.46% respectively, when their original or actual grid space (30 m) is used, while there are 75.07%, 74.88% and 75.93% areas respectively when their grid space is 330 m (Fig. 9). Five other categories show a decreased area with an increase in the size of the grid space. In the category of 5–10 t ha^{-1} yr^{-1} of soil erosion, the affected area covers 13.97%, 15.85% and 13.70% in 30 m grid space and 11.24%, 11.17% and 10.64% in 330 m grid space respectively in SRTM, ASTER and CARTOSAT. Similarly, the affected areas are 11.08%, 10.59% and 11.06% in 30 m grid space and 6.64%, 6.77% and 6.32% in 330 m grid space in 11–20 t ha^{-1} yr^{-1} rate of soil erosion respectively in SRTM, ASTER and CARTOSAT. In the category of 21–40 t ha^{-1} yr^{-1}, areas decreased from 7.62%, 6.29% and 8.05% to 3.87%, 3.87% and 3.77% using 330 m grid space in case of 30 m SRTM, ASTER and CARTOSAT

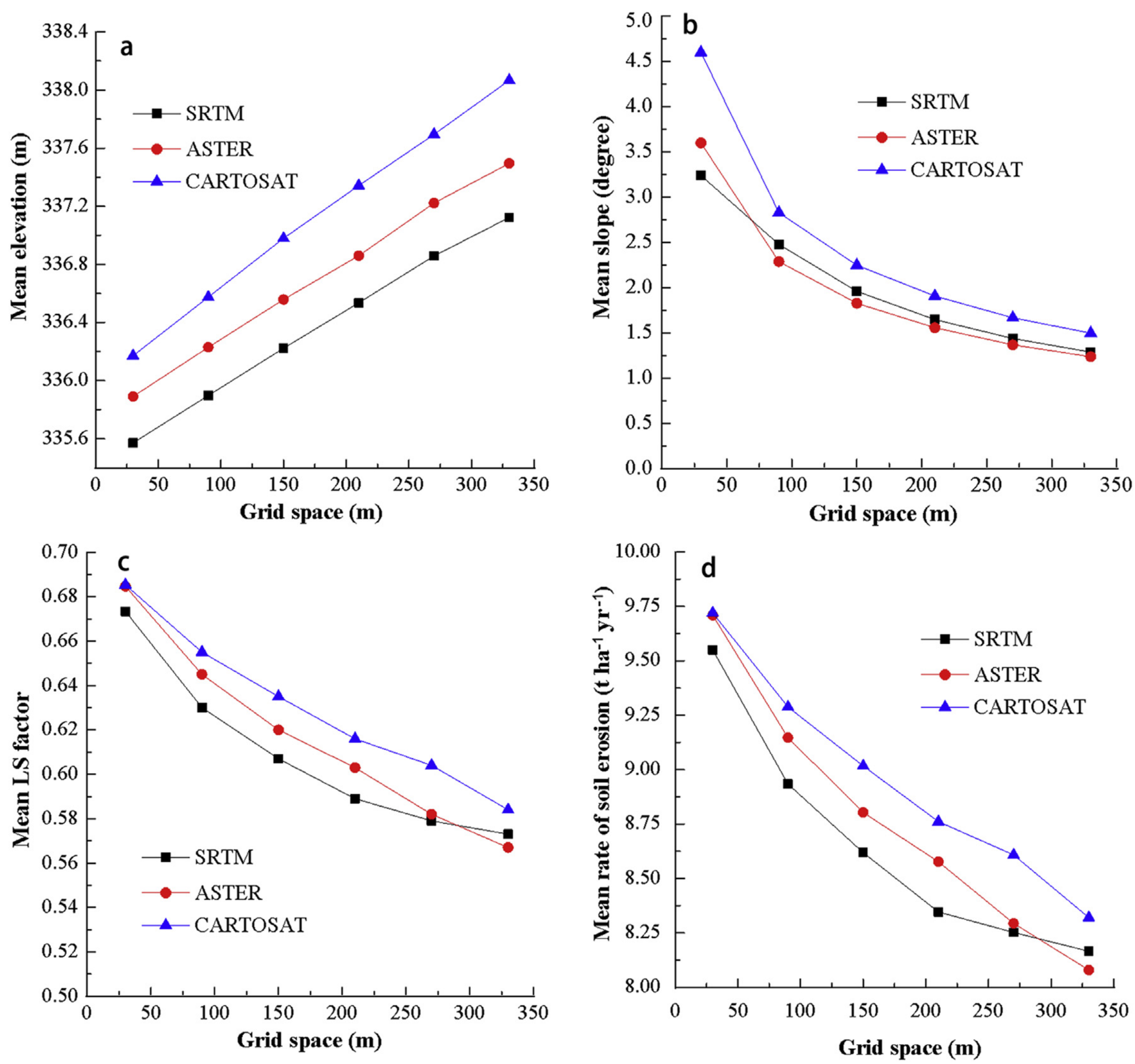

Figure 8. Comparison of the various grid space in different DEMs for (a) mean elevation, (b) mean slope, (c) mean LS factor and (d) mean rate of soil erosion.

respectively. In the category of 41–80 and >80 t ha^{-1} yr^{-1} of soil erosion, the areas show 4.66%, 3.30% and 5.38% and 3.94%, 2.17% and 5.35% in 30 m grid space and 1.76%, 1.77% and 1.74% and 1.41%, 1.51% and 1.37% in 330 m grid space respectively in SRTM, ASTER and CARTOSAT DEMs.

4.4. Spatial variation of soil erosion rate

The SRTM DEM with better accuracy is used for calculating the rate of soil erosion with a different grid space. The soil erosion rate is observed to be higher in the northern and southern boundary area, where the elevation and slope are high. On the eastern side, erosion rate is low (<5 t ha^{-1} yr^{-1}) due to low slopes. In the grid space of 30 m, little variation in erosion is identified. Variation of erosion rate is generalized when the grid space of DEM increases. It is more prominent in low slope areas where variation is even less. Areas affected by higher erosion rates in high resolution are observed to be affected by lower erosion rates in the aggregated DEMs, which is because of decreased slope and LS factor in aggregated DEMs, results in the

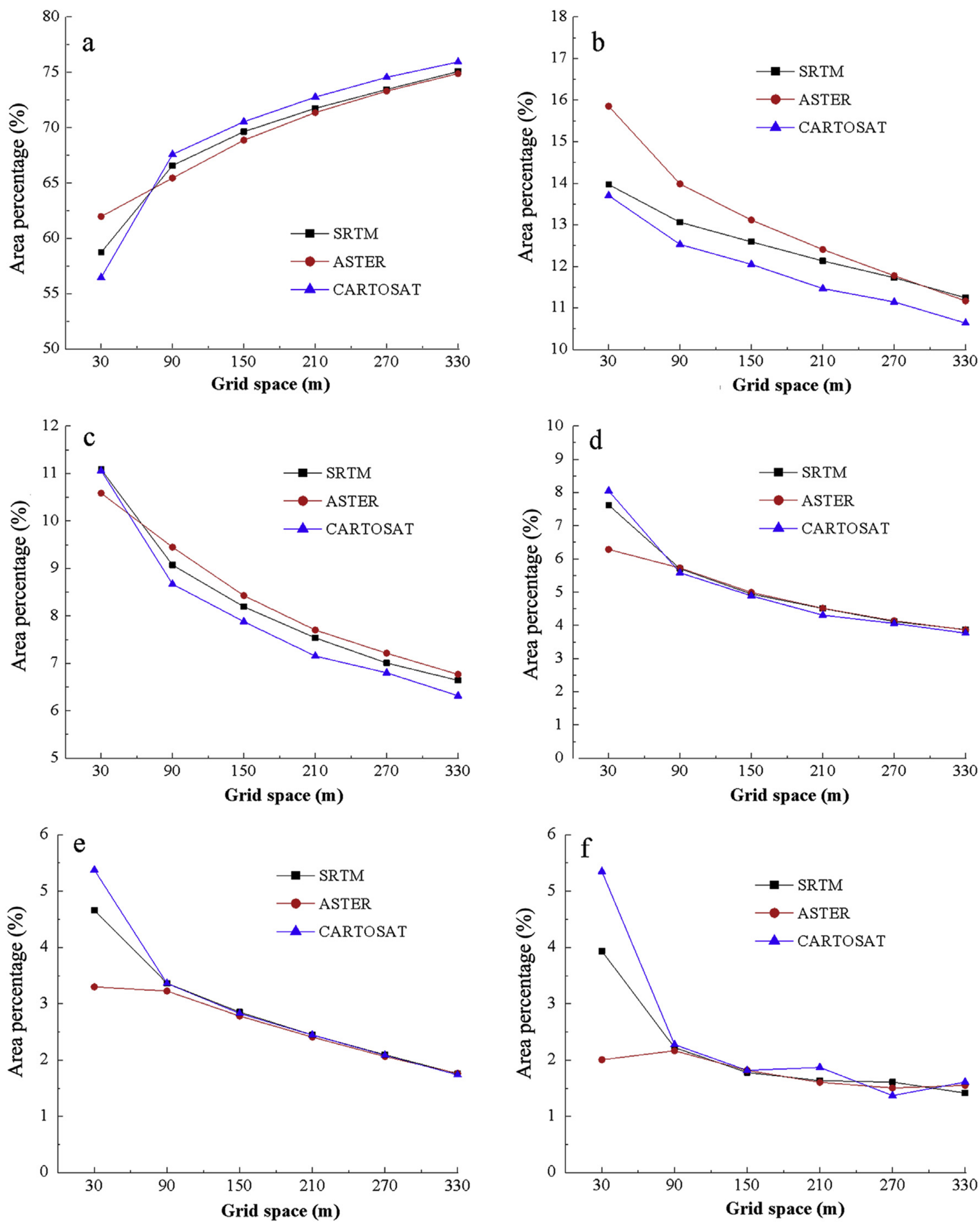

Figure 9. Change of area in different category of soil erosion rate with grid space, (a) <5 t ha^{-1} yr^{-1}, (b) 5–10 t ha^{-1} yr^{-1}, (c) 11–20 t ha^{-1} yr^{-1}, (d) 21–40 t ha^{-1} yr^{-1}, (e) 41–80 t ha^{-1} yr^{-1} and (f) >80 t ha^{-1} yr^{-1}.

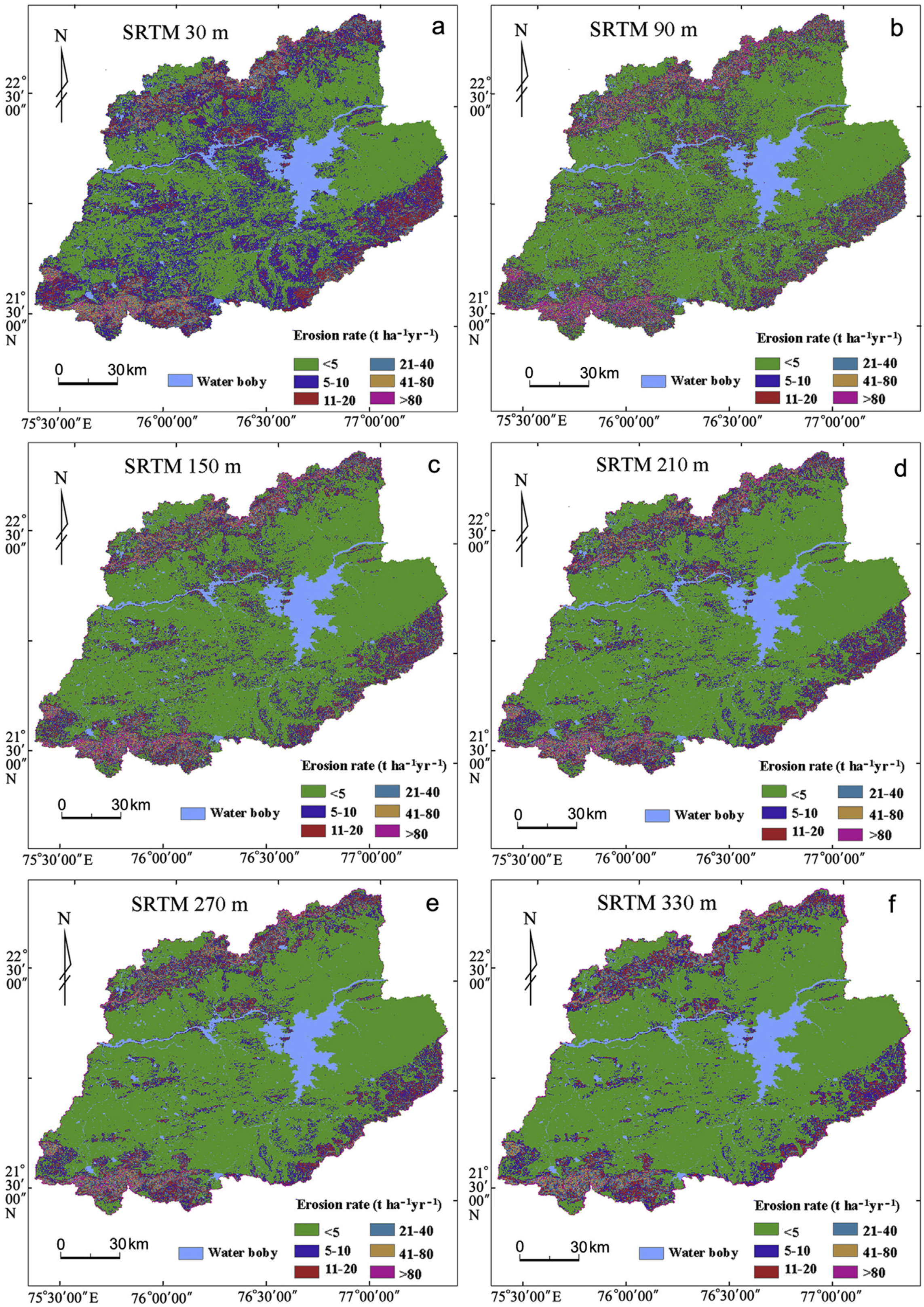

Figure 10. Soil erosion rate using different grid space of SRTM DEM.

more generalized pattern due to increased grid space. Therefore, the area of higher category of erosion rates reduces when the grid space of the DEM is high. Slight variation in the erosion rate is clearly identified in the soil erosion map using actual grid space of DEMs. Variation in erosion rate is observed to reduce gradually using higher grid space of DEMs. Areas under a discrete type of erosion rate are found to have transferred into <5 t ha^{-1} yr^{-1} category using large grid space of DEMs (Fig. 10). Similar studies with the SRTM and ASTER DEMs are carried out by Lin et al. (2013), who considered DEM as an important parameter for the models of environmental risk assessment and also as significant sources of uncertainty. Few previous studies show impacts of different DEMs with original resolutions (Cho and Lee, 2001; Di Luzio et al., 2005; Dixon and Earls, 2009), but the comparison is within a few DEMs of different resolutions. Mondal et al. (2016) used open source DEMs of different resolution and ascertained their effects on soil erosion and reports that fine resolution SRTM 30 gives better results with less uncertainty than others. In all the studies, there is a decreased effect with the coarser resolution, which is similar to the present study. According to Lin et al. (2013), the ASTER DEM has not performed better than the SRTM for various data sources, although it has comparatively higher vertical accuracy and smaller grid size, is consistent with the present study. In all these studies, there is a decrease in the mean slope with coarser resolution. Study with DEM aggregation and use in the soil erosion model USLE shows a gradual decrease in the erosion due to increased grid size by Wu et al. (2005), similar to the results of this study. However, only one DEM and its aggregation is used to analyse its effects on soil erosion. The results discussed above show the impact of the grid size of DEMs on the variation of topography determined by LS factor, which is derived from DEM.

5. Conclusion

The present study represents uncertainties of soil erosion modelling by RUSLE using original and aggregated grid space of SRTM, ASTER and CARTOSAT DEMs. The study shows a very essential aspect in the soil erosion modelling, which can vary spatially due to the difference in the elevation factor. The original, high resolution (30 m) and increased grid space of open source DEMs are used to show the uncertainty in soil erosion modelling. The results indicate that the SRTM DEM performs better than the ASTER and the CARTOSAT DEMs in assessing the accuracy. With the increased resolution also, SRTM shows better performance. This study is different from some of the recently published papers on the effect of DEM resolution on accuracy of soil erosion modelling (Liu et al., 2011; Lin et al., 2013). Sometimes, the grid space of the DEM is converted to large grid space for a particular modelling to obtain certain benefits by the users, and they might not be aware of the uncertainty of grid space conversion for modelling. The current study is an effort to illustrate and analyse uncertainties of the model outputs to aware the researchers regarding the use of open source DEMs. In case of the soil erosion modelling, finer resolution gives better results, while increased grid space gives a generalized result. However, resampling to smaller grid size might prove better, but that will also depend on the accuracy of the original grid size. The researchers should know about the error of the model output introduced by the original and increased grid space size of the DEM. The results obtained in this study may vary in different study areas, but DEMs with higher accuracy (LiDAR DEM, planimetric survey DEM, aerial photo DEM) will give more accurate results and will reduce the uncertainty.

Acknowledgement

The authors are thankful to the National Remote Sensing Centre (NRSC) for the satellite data and CARTOSAT DEM, Indian Meteorological Department (IMD) for the rainfall data, National Bureau of Soil Science (NBSS) for soil data and to the Central Water Commission (CWC) for observed sediment load data. The authors also show gratitude to the Council of Scientific & Industrial Research (CSIR) for financial assistance in the research. Authors are thankful to the Trade and Industry of Japan (METI) and the National Aeronautics and Space Administration (NASA) for the ASTER DEM. The authors are also thankful to the United States Geological Survey (USGS) for providing SRTM DEM. Authors are also grateful to the reviewers for improving the quality of the manuscript.

References

Adhikary, P.P., Tiwari, S.P., Mandal, D., Lakaria, B.L., Madhu, M., 2014. Geospatial comparison of four models to predict soil erodibility in a semi-arid region of Central India. Environmental Earth Sciences 72 (12), 5049–5062.

Alice, S., Christian, P., 2003. Erosion extension of indurate volcanic soils of Mexico by aerial photographs and remote sensing analysis. Geoderma 117, 367–375.

Barrow, C.J., 1991. Land Degradation. Cambridge University Press, Cambridge.

Chaplot, V., 2005. Impact of DEM mesh size and soil map scale on SWAT runoff, sediment, and NO_3–N loads predictions. Journal of Hydrology 312 (1–4), 207–222.

Chen, T., Niu, R.Q., Li, P.X., Zhang, L.P., Du, B., 2011. Regional soil erosion risk mapping using RUSLE, GIS, and remote sensing: a case study in Miyun Watershed, North China. Environmental Earth Sciences 63, 533–541.

Cho, S.M., Lee, M., 2001. Sensitivity considerations when modeling hydrologic processes with digital elevation model. Journal of the American Water Resources Association 37 (4), 931–934.

Dabral, P.P., Baithuri, N., Pandey, A., 2008. Soil erosion assessment in a hilly catchment of North Eastern India using USLE, GIS and remote sensing. Water Resources Management 22 (12), 1783–1798.

Di Luzio, M., Arnold, J.G., Srinivasan, R., 2005. Effect of GIS data quality on small watershed stream flow and sediment simulations. Hydrological Processes 19 (3), 629–650.

Dixon, B., Earls, J., 2009. Resample or not?! Effects of resolution of DEMs in watershed modeling. Hydrological Processes 23 (12), 1714–1724.

Duhan, D., Pandey, A., 2015. Statistical downscaling of temperature using three techniques in the Tons River basin in Central India. Theoretical and Applied Climatology 121, 605–622.

Favey, E., Geiger, A., Gudmundsson, G.H., Wehr, A., 2003. Evaluating the potential of an airborne laser-scanning system for measuring volume changes of glaciers. Geografiska Annaler: Series A, Physical Geography 81 (4), 555–561.

Feng, X.M., Wang, Y.F., Chen, L.D., Fu, B.J., Bai, G.S., 2010. Modeling soil erosion and its response to land–use change in hilly catchments of the Chinese loess plateau. Geomorphology 118, 239–248.

Fu, B.J., Zhao, W.W., Chen, L.D., Zhang, Q.J., Lü, Y.H., Gulinck, H., Poesen, J., 2005. Assessment of soil erosion at large watershed scale using RUSLE and GIS: a case study in the Loess Plateau of China. Land Degradation & Development 16, 73–85.

Hasan, R.N., Mallick, J., Devi, L.M., Siddiqui, M.A., 2013. Multi-temporal annual soil loss risk mapping employing revised universal soil loss equation (RUSLE) model in Nun Nadi Watershed, Uttrakhand (India). Arabian Journal of Geosciences 6, 4045–4056.

Hohle, J., 2009. DEM generation using a digital large format frame camera. Photogrammetric Engineering & Remote Sensing 75 (1), 87–93.

Jain, S.K., Kumar, S., Varghese, J., 2001. Estimation of soil erosion for a Himalayan watershed using GIS technique. Water Resources Management 15 (1), 41–54.

Kervyn, F., 2001. Modeling topography with SAR interferometry: illustrations of a favourable and less favourableenvironment. Computer & Geoscience 27, 1039–1050.

Kundu, S., Mondal, A., Khare, D., Mishra, P.K., Shukla, R., 2014. Shifting shoreline of Sagar Island Delta, India. Journal of Maps 10 (4), 612–619.

Li, X.S., Wu, B.F., Wang, H., Zhang, J., 2011. Regional soil erosion risk assessment in Haihe Basin. Journal of Remote Sensing 15, 372–387.

Lin, S., Jing, C., Coles, N.A., Chaplot, V., Moore, N.J., Wu, J., 2013. Evaluating DEM source and resolution uncertainties in the Soil and Water Assessment Tool. Stochastic Environmental Research and Risk Assessment 27 (1), 209–221.

Liu, H., Kiesel, J., Hörmann, G., Fohrer, N., 2011. Effects of DEM horizontal resolution and methods on calculating the slope length factor in gently rolling landscapes. CATENA 87 (3), 368–375.
Mallick, J., Alashker, Y., Mohammad, S.A.D., Ahmed, M., Hasan, M.A., 2014. Risk assessment of soil erosion in semi-arid mountainous watershed in Saudi Arabia by RUSLE model coupled with remote sensing and GIS. Geocarto International 29 (8), 915–940.
McCool, D.K., Foster, G.R., Mutchler, C.K., Meyer, L.D., 1987. Revised slope steepness factor for the universal Soil Loss Equation. Transactions of the ASABE 30 (5), 1387–1396.
Mondal, A., Khare, D., Kundu, S., Meena, P.K., Mishra, P.K., Shukla, R., 2014. Impact of climate change on future soil erosion in different slope, land use, and soil-type conditions in a part of the Narmada River Basin, India. Journal of Hydrologic Engineering 20 (6). http://dx.doi.org/10.1061/(ASCE)HE.1943-5584.0001065. C5014003.
Mondal, A., Khare, D., Kundu, S., 2016. Uncertainty analysis of soil erosion modeling using different resolution of open source DEMs. Geocarto International. http://dx.doi.org/10.1080/10106049.2016.1140822.
Mukherjee, S., Mukherjee, S., Garg, R.D., Bhardwaj, A., Raju, P.L.N., 2013a. Evaluation of topographic index in relation to terrain roughness and DEM grid spacing. Journal of Earth System Science 122 (3), 869–886.
Mukherjee, S., Joshi, P.K., Mukherjee, S., Ghosh, A., Garg, R.D., Mukhopadhyay, A., 2013b. Evaluation of vertical accuracy of open source Digital Elevation Model (DEM). International Journal of Applied Earth Observation and Geoinformation 21, 205–217.
Narayana, D.V, Babu, R., 1983. Estimation of soil erosion in India. Journal of Irrigation and Drainage Engineering 109 (4), 419–434.
Nash, J., Sutcliffe, J.V., 1970. River flow forecasting through conceptual models part I—a discussion of principles. Journal of Hydrology 10 (3), 282–290.
NBSS, 1996. Soils of Madhya Pradesh for Optimizing Land Use. National Bureau of Soil Survey and Land Use Planning (Indian Council of Agricultural Research). Department of Agriculture, Govt. of Madhya Pradesh, Bhopal. NBSS Publ. 59b, ISBN 81-85460-32-9.
NBSS, 1999. Soil Series of Madhya Pradesh. National Bureau of Soil Survey and Land Use Planning (Indian Council of Agricultural Research). Department of Agriculture, Govt. of Madhya Pradesh, Bhopal. NBSS Publ. 78 (ISBN No: 81-85460-53-1 and ISBN No. 9788185460536).
Pan, J., Wen, Y., 2014. Estimation of soil erosion using RUSLE in Caijiamiao watershed, China. Natural Hazards 71 (3), 2187–2205.
Pandey, A., Chowdary, V.M., Mal, B.C., 2007. Identification of critical erosion prone areas in the small agricultural watershed using USLE, GIS and remote sensing. Water Resources Management 21 (4), 729–746.
Pandey, A., Mathur, A., Mishra, S.K., Mal, B.C., 2009. Soil erosion modeling of a Himalayan watershed using RS and GIS. Environmental Earth Sciences 59 (2), 399–410.
Prasannakumar, V., Vijith, H., Abinod, S., Geetha, N., 2012. Estimation of soil erosion risk within a small mountainous sub-watershed in Kerala, India, using Revised Universal Soil Loss Equation (RUSLE) and geo-information technology. Geoscience Frontiers 3 (2), 209–215.
Prasuhn, V., Liniger, H., Gisler, S., Herweg, K., Candinas, A., Clément, J.P., 2013. A high-resolution soil erosion risk map of Switzerland as strategic policy support system. Land Use Policy 32, 281–291.
Quiquerez, A., Chevigny, E., Allemand, P., Curmi, P., Petit, C., Grandjean, P., 2014. Assessing the impact of soil surface characteristics on vineyard erosion from very high spatial resolution aerial images (Côte de Beaune, Burgundy, France). CATENA 116, 163–172.
Renard, K.G., Foster, G.R., Weesies, G.A., Porter, J.P., 1991. RUSLE revised universal soil loss equation. Journal of Soil and Water Conservation 46, 30–33.
Saha, S.K., Pande, L.M., 1993. Integrated approach towards soil erosion inventory for environmental conservation using satellite and agro-meteorological data. Asia-Pacific Remote Sensing 5, 21–28.
Schenk, T., 1996. Digital aerial triangulation. Archives of Photogrammetry and Remote Sensing 31 (B3), 735–745.
Sun, G., Ranson, K.J., Kharuk, V.I., Kovacs, K., 2003. Validation of surface height from shuttle radar topography mission using shuttle laser altimeter. Remote Sensing of Environment 88, 401–411.
Van der Knijff, J., Jones, R.J.A., Montanarella, L., 1999. Soil Erosion Risk Assessment in Italy (p. 52). European Soil Bureau, European Commission.
Wilson, J.P., Gallant, J.C., 2000. Secondary topographic attributes. In: Wilson, J.P., Gallant, J.C. (Eds.), Terrain Analysis: Principles and Applications. John Wiley and Sons, New York, pp. 87–131.
Wischmeier, W.H., Smith, D.D., 1978. Predicting Rainfall Erosion Losses. A Guide to Conservation Planning. USDA Agricultural Handbook No. 537, Washington, DC.
Wu, S., Li, J., Huang, G., 2005. An evaluation of grid size uncertainty in empirical soil loss modeling with digital elevation models. Environmental Modeling and Assessment 10, 33–42. http://dx.doi.org/10.1007/s10666-004-6595-4.
Xu, Y.Q., Shao, X.M., Kong, X.B., Peng, J., Cai, Y.L., 2007. Adapting the RUSLE and GIS to model soil erosion risk in a mountains karst watershed, Guizhou Province, China. Environmental Monitoring and Assessment 141, 275–286.

Please cite this article in press as: Mondal, A., et al., Uncertainty of soil erosion modelling using open source high resolution and aggregated DEMs, Geoscience Frontiers (2016), http://dx.doi.org/10.1016/j.gsf.2016.03.004